

# Online Time and Energy Resolved Flux Measurements of sub-MeV Charged Particles with the Zirè Low Energy Module (LEM) on the NUSES Space Mission

**Riccardo Nicolaidis<sup>a,b,\*</sup> on behalf of the NUSES collaboration**

<sup>a</sup>*University of Trento - Physics Department,  
Via Sommarive, 14, 38123 Povo TN, Italia*

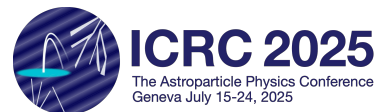
<sup>b</sup>*Trento Institute of Fundamental Physics and Applications (TIFPA-INFN),  
Via Sommarive, 14, 38123 Povo TN, Italia*

*E-mail: [riccardo.nicolaidis@unitn.it](mailto:riccardo.nicolaidis@unitn.it)*

Observing and monitoring low-energy charged particles—from sub-MeV up to tens of MeVs—has become increasingly important for several reasons, impacting various fields of science. These range from radiation protection and the study of magnetosphere–lithosphere interactions to investigations of space weather and the interplay between the heliospheric environment and the magnetosphere. To address this wide array of scientific objectives, the Low Energy Module (LEM) onboard the NUSES space mission has been developed.

NUSES is a planned space mission designed to test innovative approaches for studying low-energy cosmic rays, gamma rays, astrophysical neutrinos, space weather phenomena, and models of magnetosphere–ionosphere–lithosphere coupling. The NUSES satellite carries two payloads: Terzina and Zirè. Zirè, which measures protons and electrons up to a few hundred MeV, incorporates the LEM, a compact particle spectrometer mounted directly on the satellite’s external top panel. The LEM is dedicated to measure fluxes of low-energy electrons (0.1–7 MeV) and protons (3–50 MeV) in the low-Earth orbit environment. Its compact design and limited acceptance enable event-based particle identification even in high-radiation regions such as the South Atlantic Anomaly and the inner Van Allen belt, where electron fluxes can reach approximately  $10^6 \text{ cm}^{-2} \text{ s}^{-1} \text{ sr}^{-1}$ . The innovative features of the LEM include its extremely compact design—fitting within a  $10 \times 10 \times 10 \text{ cm}^3$  volume—and its active collimation technique, which effectively mitigates the challenges of multiple scattering (that typically prevent the use of standard tracking techniques) at low energies. In this contribution, we present the geometry and detection concept of the detector flight model, its expected scientific performance, the data products that will be available in orbit.

39th International Cosmic Ray Conference (ICRC2025)  
15–24 July 2025  
Geneva, Switzerland



\*Speaker

## 1. The NUSES Mission and the Role of LEM

The NUSES space mission is designed to explore low-energy cosmic rays, gamma rays, and astrophysical neutrinos through innovative detection concepts [1]. Its launch is scheduled for early 2027 into a Sun-synchronous low-Earth orbit at approximately 530 km altitude, with a nominal duration of at least three years.

NUSES will host two scientific payloads: Terzina, an optical telescope aimed at detecting Cherenkov light from Extensive Air Showers (EAS) [2, 3], and Zirè, a particle detector focused on the detection of protons, electrons, and photons over a broad energy range [4, 5]. As a sub-detector of Zirè, the Low Energy Module (LEM) extends the instrument's sensitivity toward lower energies, enabling the detection of electrons from 0.1 to 7 MeV and protons from 3 to 50 MeV [6, 7].

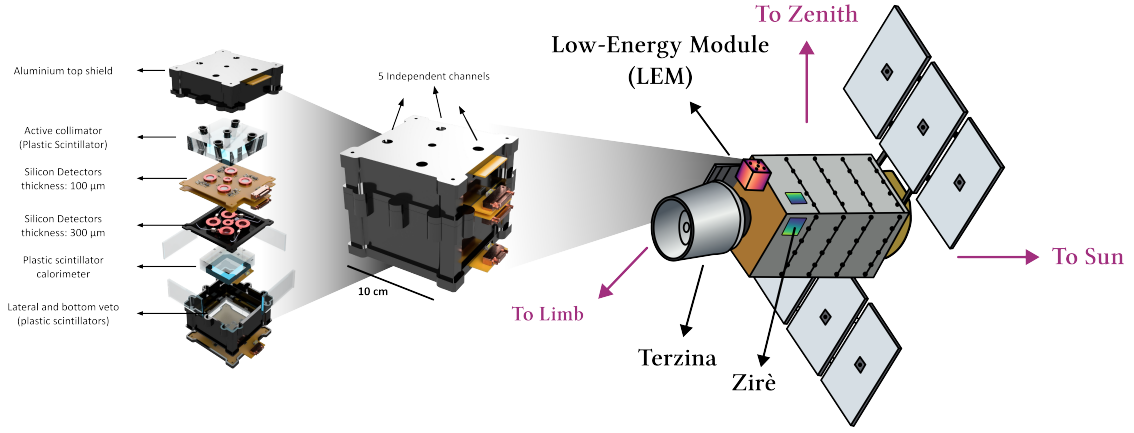


**Figure 1:** Exploded view of the Low Energy Module (LEM) and its integration on the NUSES satellite. LEM is a compact particle spectrometer ( $10 \times 10 \times 10 \text{ cm}^3$ ) mounted on the top external panel of the satellite. The figure shows the internal detector layers: active collimators, segmented silicon sensors, scintillator tiles, and readout electronics. The modular design enables event-by-event energy and time-resolved measurements of electrons and protons in the MeV range.

LEM is a compact ( $10 \times 10 \times 10 \text{ cm}^3$ ) particle spectrometer employing a novel active collimation technique and a  $\Delta E$ – $E$  detection scheme (described in Section 2), which allow for accurate event-by-event particle identification even in high-flux environments such as the South Atlantic Anomaly (SAA).

The scientific objectives of LEM include monitoring trapped particle precipitation from the Van Allen Belts (VABs) and investigating its possible correlations with seismic and volcanic activities. Several electromagnetic phenomena—triggered by solar storms, atmospheric discharges, or seismic events—may alter the radiation belt configuration, inducing particle precipitations. These processes are central to Lithosphere–Atmosphere–Ionosphere–Magnetosphere (LAIM) interaction models [8]. Past studies have reported temporal correlations between low-energy particle bursts and large seismic events [9], motivating the need for precise flux measurements in the MeV range as a potential tool for identifying seismic precursors.

Additionally, LEM will operate during the maximum of the 11-year solar cycle, contributing to the monitoring of Solar Flares (SFs) and Coronal Mass Ejections (CMEs) [10]. These observations

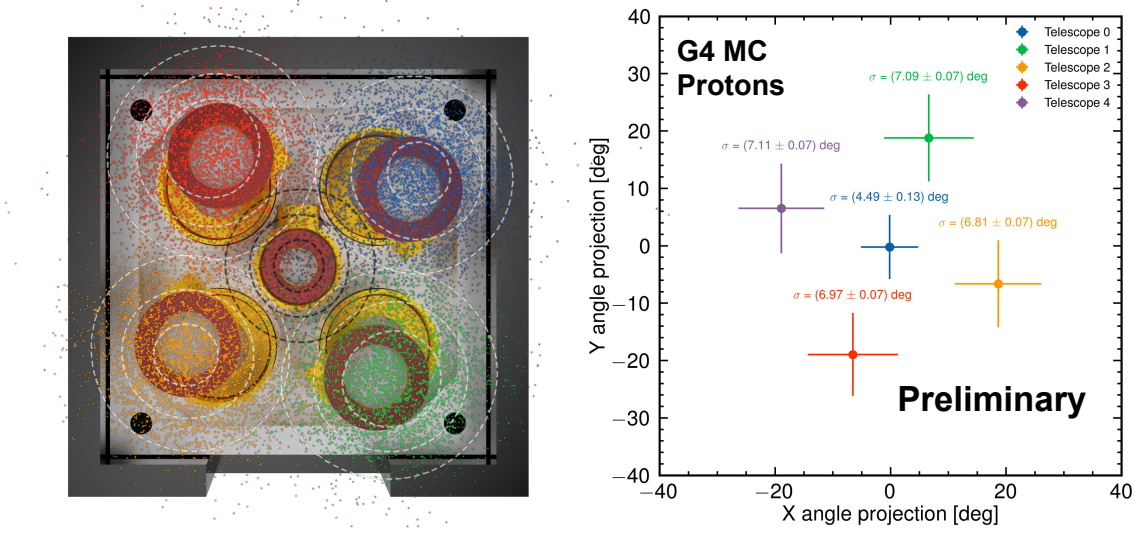


**Figure 2:** Left: angular distribution of reconstructed proton directions from Geant4 simulations, projected onto the X–Y plane. Each color corresponds to one of the five  $\Delta E$ – $E$  telescopes in the LEM. The circular patterns reflect the geometrical acceptance defined by the drilled active collimator layer. Right: mean reconstructed angle and angular resolution ( $\sigma$ ) for each telescope.

will provide new insights into particle acceleration mechanisms and space weather conditions in the near-Earth environment.

As illustrated in Fig. 1, the LEM is composed of multiple detection layers—including silicon sensors and scintillators—enclosed in a  $10 \times 10 \times 10 \text{ cm}^3$  mechanical structure and mounted on the top panel of the NUSES satellite.

## 2. The LEM Detection Concept

The Low Energy Module (LEM) is designed to perform time-resolved measurements of the direction, energy, and composition (charge and mass) of charged particles in low-Earth orbit. Its mechanical structure and internal components are shown in Fig. 1.

At sub-MeV energies, conventional tracking techniques based on silicon strip or pixel detectors become ineffective due to dominant multiple Coulomb scattering. To overcome this limitation, LEM adopts the active collimation technique [6], which employs a 1 cm thick plastic scintillator tile with five cylindrical channels drilled along fixed directions. Charged particles entering the detector at the predefined angles are able to pass through the collimator without significant energy loss, while particles from other directions interact with the scintillator and can be vetoed. This method enables event-by-event directional reconstruction without requiring full tracking. The angular responses of the five  $\Delta E$  –  $E$  telescopic configurations are displayed in Fig. 2, with a resolution of about  $7^\circ$  for protons and up to  $15^\circ$  for electrons, the latter affected by scattering in the upper aluminum shield.

Energy measurement and particle identification are performed using five independent  $\Delta E$ – $E$  telescopes, each composed of a  $100 \mu\text{m}$  thick surface barrier silicon detector (Ametek/ORTEC [11]) followed by a  $300 \mu\text{m}$  thick passivated implanted planar silicon (PIPS) detector (Mirion Technolo-

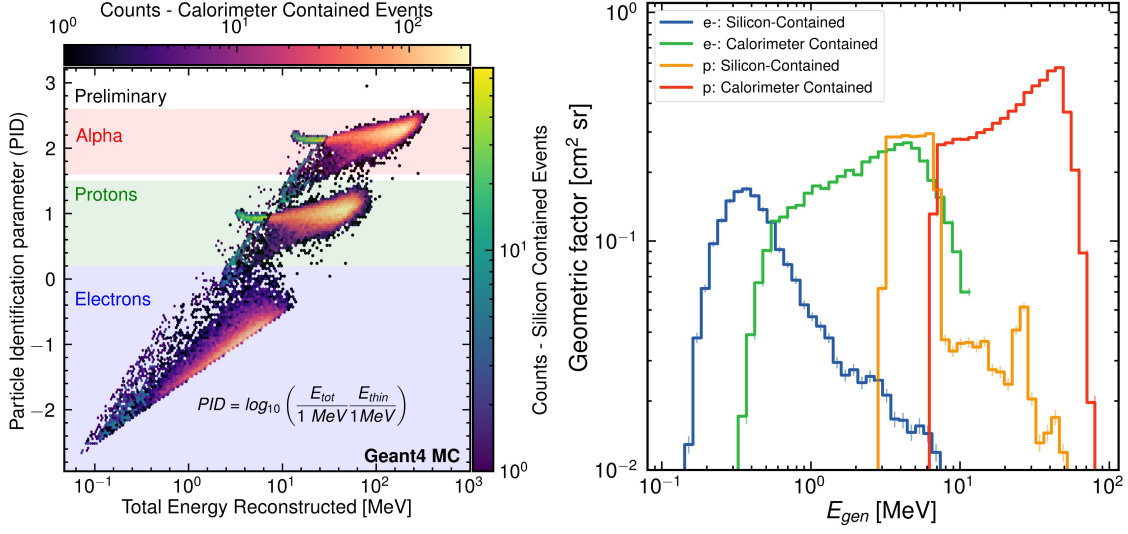


**Figure 3:** Left: particle identification parameter (PID) as a function of the total reconstructed energy from Geant4 Monte Carlo simulations. The PID is defined as  $\log_{10} \left( \frac{E_{\text{tot}}}{1 \text{ MeV}} \cdot \frac{E_{\text{thin}}}{1 \text{ MeV}} \right)$ , and enables clear separation between electrons, protons, and alpha particles. The overlaid heatmaps represent the number of events fully contained in the silicon detectors (right colorbar) and in the calorimeter (top colorbar). Right: geometric factor as a function of the generated particle energy for electrons and protons, distinguishing between events fully contained in the silicon layers and those reaching the calorimeter. The curves demonstrate the complementary acceptance of the two subsystems across the LEM’s target energy range.

gies [12]). These telescopes are aligned with the active collimator channels, ensuring that only particles with known trajectories are accepted.

In the non-relativistic regime, the total kinetic energy is given by  $E_{\text{tot}} \approx \frac{1}{2}mv^2$ , while the energy deposited in the thin  $\Delta E$  layer scales as  $E_{\text{thin}} \propto Z^2/v^2$ , where  $Z$  is the particle charge and  $v$  its velocity. Their product,  $E_{\text{tot}}E_{\text{thin}} \propto Z^2m$ , is approximately independent of velocity, and can be used to infer both charge and mass. While this approximation breaks down for relativistic electrons, their low mass ensures clear separation in the particle identification space. Figure 3 (left panel) shows the distribution of the PID parameter as a function of total energy, obtained from Geant4 simulations.

To extend the measurable energy range beyond the silicon detectors, a 2 cm thick plastic scintillator is placed below each telescope, acting as a calorimeter. Events depositing energy in this layer can be used to reconstruct higher energy particles. The overall containment efficiency and geometrical acceptance for calorimeter and silicon events are also shown in Fig. 3 (right panel).

Additional plastic scintillator panels are placed laterally and beneath the detector, acting as veto layers to reject crossing or not fully contained events. The entire LEM structure is enclosed in a 7 mm thick drilled aluminum shield, designed to suppress spurious activations in high-background regions such as the SAA and polar caps.

### 3. Acquisition Modes and Event Handling

To ensure continuous coverage for the scientific observation through diverse radiation environments, the LEM detector employs an adaptive data acquisition (DAQ) system featuring two



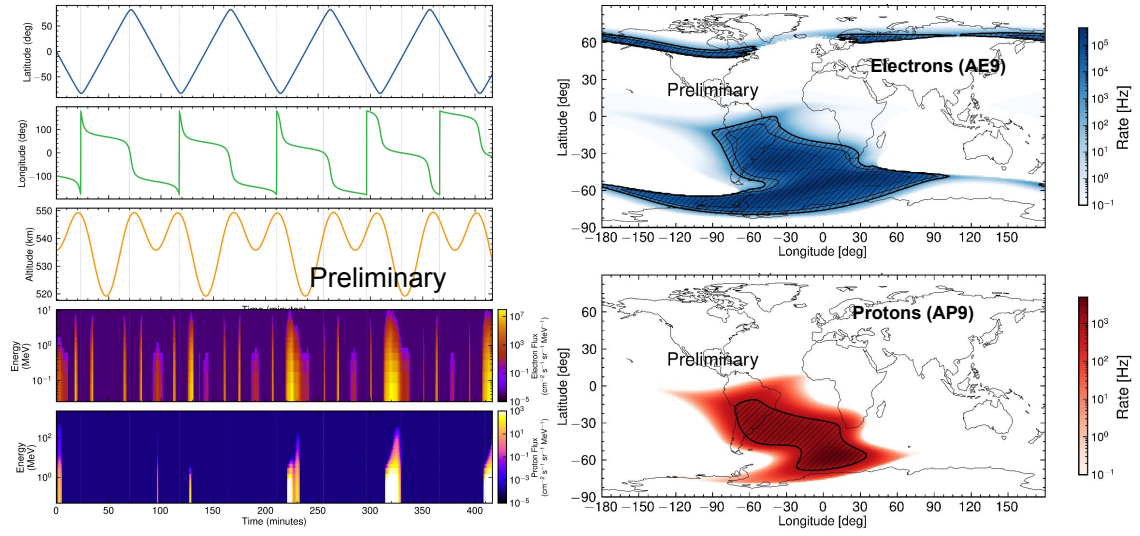


**Figure 4:** Left: simulated orbital parameters and expected fluxes along one orbit of the NUSES satellite. From top to bottom: latitude, longitude, and altitude profiles as a function of time (first three panels); differential electron flux (fourth panel) and proton flux (fifth panel) along the orbit, based on AE9 and AP9 models, respectively. Enhanced fluxes are observed in correspondence with the South Atlantic Anomaly (SAA) and auroral regions. Right: global maps of particle rates integrated over energy and pitch angle, as predicted by AE9 (electrons, top) and AP9 (protons, bottom) at LEM's orbital altitude. The maps highlight the high-radiation regions such as the SAA and the outer radiation belts, where count rates can reach several kHz.

operational modes. In *list mode*, all triggered events are acquired individually and transmitted as fixed-length packets containing calibrated amplitudes, timestamps, and quality flags from all detector channels. This mode preserves full pulse-shape information and is used when the trigger rate remains below a configurable threshold (nominally 1 kHz), typically in low-background regions.

When the particle rate exceeds this threshold, as expected in regions such as the SAA or the auroral zones, the instrument switches to *histogram mode*. In this configuration, the onboard firmware projects the event observables onto a logarithmic energy scale and accumulates two-dimensional histograms of energy versus particle identification parameters. These compact data packets are transmitted once per second, reducing bandwidth usage while maintaining scientific data quality.

This dual-mode architecture allows the LEM to operate efficiently under both quiet and high-rate conditions without exceeding telemetry constraints. The expected temporal and spatial distribution of high-rate regions requiring histogram mode is shown in Fig. 4, along with other orbital parameters, where shaded areas in the right panel of the figure indicate zones in which the expected event rate surpasses 1 kHz.

#### 4. Conclusion

The LEM of the Zirà payload on board the NUSES mission has been designed to provide time- and energy-resolved measurements of low-energy charged particles in low-Earth orbit. Its compact

design, active collimation technique, and multi-layer  $\Delta E-E$  detection architecture enable precise identification of electrons and protons in a challenging radiation environment.

LEM's dual acquisition strategy, combining event-based list mode and histogram-based compression, ensures continuous data collection even in the high-flux regions such as the SAA. Simulation results and laboratory characterizations confirm the detector's ability to operate with energy thresholds below 30 keV and angular resolution down to a few degrees. These capabilities will allow LEM to contribute significantly to the study of space weather, magnetospheric dynamics, and particle precipitation potentially associated with seismic and volcanic activities. The payload is currently undergoing final integration and test campaigns, with flight operations scheduled to begin after launch in late 2026.

## Acknowledgements

NUSES is funded by the Italian Government (CIPE n. 20/2019), by the Italian Ministry of Economic Development (MISE reg. CC n. 769/2020), by the Italian Space Agency (CDA ASI n. 15/2022), by the European Union NextGenerationEU under the MUR National Innovation Ecosystem grant ECS00000041 - VITALITY - CUP D13C21000430001 and by the Swiss National Foundation (SNF grant n. 178918). This study was carried out also in collaboration with the Ministry of University and Research, MUR, under contract n. 2024-5-E.0 - CUP n. I53D24000060005. This research, leading to the beam test results, also received partial funding from the European Union's Horizon Europe research and innovation programme under grant agreement No. 101057511.

## Author list

M. Abdullahi<sup>a,b</sup>, R. Aloisio<sup>a,b</sup>, S. Ashurov<sup>a,b</sup>, U. Atalay<sup>a,b</sup>, F. C. T. Barbato<sup>a,b</sup>, R. Battiston<sup>d,e</sup>, M. E. Bertaina<sup>f,g</sup>, E. Bissaldi<sup>c,h</sup>, D. Boncioli<sup>b,i</sup>, L. Burmistrov<sup>j</sup>, I. Cagnoli<sup>a,b</sup>, E. Casilli<sup>a,b</sup>, F. Cadoux<sup>j</sup>, A. L. Cummings<sup>m</sup>, D. Cortis<sup>b</sup>, M. D'Arco<sup>j</sup>, S. Davarpanah<sup>j</sup>, I. De Mitri<sup>a,b</sup>, G. De Robertis<sup>c</sup>, A. Di Giovanni<sup>a,b</sup>, A. Di Salvo<sup>g</sup>, L. Di Venere<sup>c</sup>, J. Eser<sup>k</sup>, Y. Favre<sup>j</sup>, S. Fogliacco<sup>a,b</sup>, G. Fontanella<sup>a,b</sup>, P. Fusco<sup>c,h</sup>, S. Garbolino<sup>g</sup>, F. Gargano<sup>c</sup>, M. Giliberti<sup>c,h</sup>, F. Guarino<sup>o,p</sup>, M. Heller<sup>j</sup>, R. Iuppa<sup>d,e</sup>, D. Kyratzis<sup>a,b</sup>, J. F. Krizmanic<sup>q</sup>, F. Licciulli<sup>c</sup>, A. Liguori<sup>c,h</sup>, F. Loparco<sup>c,h</sup>, L. Lorusso<sup>c,h</sup>, M. Mariotti<sup>s,t</sup>, M. N. Mazziotta<sup>c</sup>, M. Mese<sup>o,p</sup>, M. Mignone<sup>f,g</sup>, T. Montaruli<sup>j</sup>, R. Nicoladis<sup>d,e</sup>, F. Nozzoli<sup>d,e</sup>, A. V. Olinto<sup>n</sup>, D. Orlandi<sup>b</sup>, G. Osteria<sup>o</sup>, P. A. Palmieri<sup>f,g</sup>, B. Panico<sup>o,p</sup>, G. Panzarini<sup>c,h</sup>, D. Pattanaik<sup>a,b</sup>, L. Perrone<sup>u,v</sup>, H. Pessoa Lima<sup>a,b</sup>, R. Pillera<sup>c,h</sup>, R. Rando<sup>s,t</sup>, A. Rivetti<sup>g</sup>, V. Rizi<sup>b,i</sup>, A. Roy<sup>a,b</sup>, F. Salamida<sup>b,i</sup>, R. Sarkar<sup>a,b</sup>, P. Savina<sup>a,b</sup>, V. Scherini<sup>u,v</sup>, V. Scotti<sup>o,p</sup>, D. Serini<sup>c</sup>, D. Shledewitz<sup>d,e</sup>, I. Siddique<sup>a,b</sup>, A. Smirnov<sup>a,b</sup>, R. A. Torres Saavedra<sup>a,b</sup>, C. Trimarelli<sup>j,w</sup>, P. Zuccon<sup>d,e</sup>, S. C. Zugravel<sup>g</sup>

## Affiliations

<sup>a</sup> Gran Sasso Science Institute (GSSI), Via Iacobucci 2, I-67100 L'Aquila, Italy

<sup>b</sup> Istituto Nazionale di Fisica Nucleare (INFN) - Laboratori Nazionali del Gran Sasso, Via G. Acitelli 22, I-67100 Assergi, L'Aquila, Italy

- <sup>c</sup> Istituto Nazionale di Fisica Nucleare (INFN) - Sezione di Bari, Via Orabona 4, I-70126 Bari, Italy
- <sup>d</sup> Dipartimento di Fisica - Università di Trento, Via Sommarive 14, I-38123 Trento, Italy
- <sup>e</sup> Istituto Nazionale di Fisica Nucleare (INFN) - Sezione di Trento, Via Sommarive 14, I-38123 Trento, Italy
- <sup>f</sup> Dipartimento di Fisica - Università di Torino, Via P. Giuria 1, I-10125 Torino, Italy
- <sup>g</sup> Istituto Nazionale di Fisica Nucleare (INFN) - Sezione di Torino, Via P. Giuria 1, I-10125 Torino, Italy
- <sup>h</sup> Dipartimento di Fisica M. Merlin dell' Università e del Politecnico di Bari, Via Amendola 173, I-70126 Bari, Italy
- <sup>i</sup> Dipartimento di Scienze Fisiche e Chimiche - Università degli Studi di L'Aquila, Via Vetoio 42, I-67100 L'Aquila, Italy
- <sup>j</sup> Département de Physique Nucléaire et Corpusculaire - Université de Genève, Faculté de Science, 24 Quai Ernest-Ansermet, 1205 Genève, Switzerland
- <sup>k</sup> Columbia University, Columbia Astrophysics Laboratory, New York, NY U.S.A
- <sup>m</sup> Department of Physics and Astronomy & Astrophysics, Institute for Gravitation and the Cosmos - Pennsylvania State University, University Park, PA 16802, USA
- <sup>n</sup> Department of Astronomy and Astrophysics, University of Columbia, New York, NY, USA
- <sup>o</sup> Istituto Nazionale di Fisica Nucleare (INFN) - Sezione di Napoli, Via Cintia, I-80126 Napoli, Italy
- <sup>p</sup> Dipartimento di Fisica E. Pancini - Università di Napoli Federico II, Via Cintia, I-80126 Napoli, Italy
- <sup>q</sup> CRESST/NASA Goddard Space Flight Center, Greenbelt, MD 20771, USA
- <sup>s</sup> Dipartimento di Fisica e Astronomia - Università di Padova, I-35122 Padova, Italy
- <sup>t</sup> Istituto Nazionale di Fisica Nucleare (INFN) - Sezione di Padova, I-35131 Padova, Italy
- <sup>u</sup> Dipartimento di Matematica e Fisica "E. De Giorgi" - Università del Salento, Via per Arnesano, I-73100 Lecce, Italy
- <sup>v</sup> Istituto Nazionale di Fisica Nucleare (INFN) - Sezione di Lecce, Via per Arnesano, I-73100 Lecce, Italy
- <sup>w</sup> Now at Gran Sasso Science Institute (GSSI), Istituto Nazionale di Fisica Nucleare (INFN) - Laboratori Nazionali del Gran Sasso

## References

- [1] I. De Mitri and M. Di Santo. The NUSES space mission. *J. Phys. Conf. Ser.*, 2429(1):012007, 2023.
- [2] Roberto Aloisio et al. The Terzina instrument on board the NUSES space mission. *PoS, ICRC2023*:391, 2023.
- [3] Leonid Burmistrov. Terzina on board NUSES: A pathfinder for EAS Cherenkov Light Detection from space. *EPJ Web Conf.*, 283:06006, 2023.

- [4] G. Panzarini, F. C. T. Barbato, I. De Mitri, A. Di Giovanni, M. N. Mazziotta, R. Nicolaidis, F. Nozzoli, R. Pillera, and P. Savina. The Zirè instrument onboard the NUSES space mission. *Nucl. Instrum. Meth. A*, 1068:169794, 2024.
- [5] Ivan De Mitri and Mateo Fernandez Alonso. The Zire experiment on board the NUSES space mission. *PoS, ICRC2023*:139, 2023.
- [6] Riccardo Nicolaidis, Francesco Nozzoli, and Giancarlo Pepponi. A Compact Particle Detector for Space-Based Applications: Development of a Low-Energy Module (LEM) for the NUSES Space Mission. *Instruments*, 7(4):40, 2023.
- [7] Francesco Nozzoli and Riccardo Nicolaidis. The Low Energy Module (LEM) of the Zire payload on board the NUSES space mission. *PoS, ICRC2023*:1316, 2023.
- [8] Giulia D’Angelo, Mirko Piersanti, Roberto Battiston, Igor Bertello, Vincenzo Carbone, Antonio Cicone, Piero Diego, Emanuele Papini, Alexandra Parmentier, Piergiorgio Picozza, et al. Haiti Earthquake (Mw 7.2): Magnetospheric–Ionospheric–Lithospheric Coupling during and after the Main Shock on 14 August 2021. *Remote Sensing*, 14(21):5340, 2022.
- [9] Roberto Battiston and Vincenzo Vitale. First evidence for correlations between electron fluxes measured by NOAA-POES satellites and large seismic events. *Nucl. Phys. B Proc. Suppl.*, 243-244:249–257, 2013.
- [10] SW Kahler. Solar flares and coronal mass ejections. *Annual review of astronomy and astrophysics*, 30(1):113–141, 1992.
- [11] ORTEC/AMETEK. Silicon charged particle radiation detectors for research applications. Available at: [www.ortec-online.com](http://www.ortec-online.com) (Accessed: 2024-11-28).
- [12] Mirion Technologies. Passivated implanted planar silicon detectors®. Available at: [www.mirion.com](http://www.mirion.com) (Accessed: 2024-11-28).